Screen level temperature increase due to higher atmospheric carbon dioxide in calm and windy nights revisited

G. J. Steeneveld,[1] A. A. M. Holtslag,[1] R. T. McNider,[2] and R. A. Pielke Sr.[3]

Received 10 June 2010; revised 7 November 2010; accepted 11 November 2010; published 27 January 2011.

[1] Long-term surface observations over land have shown temperature increases during the last century, especially during nighttime. Observations analyzed by Parker (2004) show similar long-term trends for calm and windy conditions at night, and on basis of this it was suggested that the possible effect of urban heat effects on long-term temperature trends are small. On the other hand, a simplified analytic model study by Pielke and Matsui (2005) (hereinafter referred to as PM05) suggests that at night the resultant long-term temperature trends over land should depend on height and strongly on wind speed (mostly due to alterations in the rate of nocturnal cooling in the stable boundary layer (SBL)). In this paper we expand the PM05 study by using a validated atmospheric boundary layer model with elaborated atmospheric physics compared to PM05, in order to explore the response of the SBL over land to a change in radiative forcing. We find that the screen level temperature response is surprisingly constant for a rather broad range of both geostrophic wind speed (5–15 m s^{-1}) and 10 m wind (2–4.0 m s^{-1}). This is mostly due to land surface-vegetation-atmosphere feedbacks taken into account in the present study which were not considered by PM05.

Citation: Steeneveld, G. J., A. A. M. Holtslag, R. T. McNider, and R. A. Pielke Sr. (2011), Screen level temperature increase due to higher atmospheric carbon dioxide in calm and windy nights revisited, *J. Geophys. Res.*, *116*, D02122, doi:10.1029/2010JD014612.

1. Introduction

[2] Long-term air temperature increases at screen height (normally 2 m above the ground surface) is dominantly observed at night over land [*Folland et al.*, 2001]. *Parker* [2004, 2006] examined time series of worldwide temperature observations in order to understand whether the long-term temperature trend differs between windy and calm nights. He found that the globally averaged screen level temperature increase over land appears to be quantitatively the same for windy and calm nights (i.e., ~0.19 K/decade). As such it was concluded that global long-term temperature increase is apparently not obscured by urban heat island effects, since otherwise the screen level temperature increase would be smaller for stronger winds.

[3] *Pielke and Matsui* [2005] (hereinafter referred to as PM05) question the findings by *Parker* [2004]. Based on a simple conceptual boundary layer model, PM05 find that an increase in surface heat flux of 1 W m^{-2} (from −50 W m^{-2} to −49 W m^{-2} (representing an increase in downward flux from greenhouse gases, water vapor, or cloud cover, for example)) gives a screen level temperature increase of ~0.3 K for 10 m s^{-1} and ~1.7 K at 1 m s^{-1} wind speed. They also concluded that the response to the additional heat input should be height dependent. PM05 noted that since their findings showed that temperature change alterations in the nocturnal cooling rate was a function of wind speed, Parker's conclusions need further analysis and interpretation.

[4] This paper revisits this issue. First we consider the explicit assumption of fixed heat input independent of wind speed for which PM05 make their statement. Second, we discuss the simplifications of the model used by PM05. Then as an alternative, we use a high-resolution, validated, column model for the SBL coupled to the land surface to examine the vertical structure of the temperature increase by forcing the model with increased CO_2 and we assess whether this temperature increase differs for different geostrophic wind speeds ($\mathbf{V_g}$).

2. Background

[5] The atmospheric boundary layer (ABL) is the lower part of the atmosphere where the influence of the diurnal cycle over land is strongly felt. On clear nights, the temperature at the land surface falls rapidly and the air becomes cooler close to the ground than aloft; that is, the ABL is stably stratified. Apart from the large-scale dynamics (i.e., pressure gradient and Coriolis force), the physics that govern the structure of wind speed and temperature profiles is complex and involves several processes with many feedbacks (both positive and negative). These physical processes

[1] Meteorology and Air Quality Section, Wageningen University, Wageningen, Netherlands.
[2] Department of Atmospheric Science, University of Alabama in Huntsville, Huntsville, Alabama, USA.
[3] CIRES and Department of Atmospheric and Oceanic Sciences, University of Colorado at Boulder, Boulder, Colorado, USA.

0148-0227/11/2010JD014612

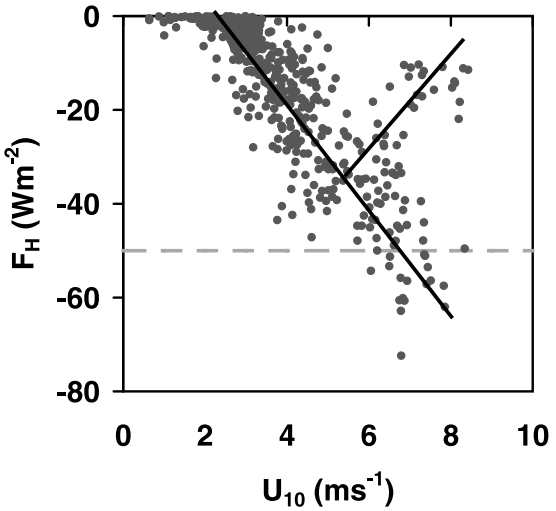

Figure 1. Observed sensible heat flux H as function of wind speed U (10 m) during the CASES-99 experiment. Observations have been selected for 2200–0700 local time and surface net radiation smaller than −50 W m^{-2} (to exclude clouds). The gray dashed line is estimate used in equation (1), and the bold lines indicate the different regimes. Observations courtesy of Oscar Hartogensis.

are turbulent mixing, radiative heat transport and the interaction with the vegetation and the underlying soil. In addition, small-scale and less well understood processes as propagating gravity waves [*Chimonas and Nappo*, 1989], drainage flows, low-level jets [*McNider and Pielke*, 1981] and intermittent turbulence [*van de Wiel et al.*, 2002] may be relevant.

[6] Turbulent mixing in the SBL is a highly nonlinear process [e.g., *McNider et al.*, 1995; *van de Wiel et al.*, 2002; *Holtslag et al.*, 2007]. Concerning the turbulent sensible heat flux (F_H (W m^{-2})), we can at least distinguish two different regimes. In the first regime increased stratification results in an increased magnitude of F_H, since F_H is proportional to the stratification in this regime. This negative feedback dominates during windy nights. Contrary, in the second regime, increased stratification inhibits turbulent mixing so strongly that the magnitude F_H decreases with increased stratification, and in the extreme case turbulence vanishes. This regime is dominant during calm nights [e.g., *Delage et al.*, 2002; *van de Wiel et al.*, 2002].

[7] In addition, we note that radiative heat transport is a complex process of absorption and emission of thermal radiation (by absorbers) between atmospheric layers, and to and from the surface. The net effect close to the surface is a cooling of the atmosphere and a smoothing of the temperature profile, but the quantitative contribution depends on the time-dependent curvature of the temperature profile and the slope of the humidity profiles [*Ha and Mahrt*, 2003; *Steeneveld et al.*, 2010].

[8] Finally, land surface cooling is the process that increases gradients of the atmospheric temperature profile. A strong and direct feedback between the surface vegetation and the underlying soil is well known [*van de Wiel et al.*, 2002]. Increased longwave cooling leads to a stronger compensating heat flux from the soil to the surface. In the case of inhibited F_H, the net radiation and the soil heat flux are the dominating contributors to the surface energy budget.

[9] The sketch above clearly illustrates that the SBL cooling and resulting temperature profile at night is highly nonlinear and a subtle balance of processes. In a first attempt at addressing the response of the SBL to changes in surface forcing, PM05 chose to use a rather simple analytical model to describe the temperature profile at night which was original proposed by *Stull* [1983, 2000]. In that model, the potential temperature profile $\theta(z)$ is described as function of height z and a SBL height scale H_e by using:

$$\theta(z) = \Delta\theta_s e^{-\frac{z}{H_e}} = \frac{\int F_H dt}{\rho C_p H_e} e^{-\frac{z}{H_e}}. \quad (1)$$

Here $\Delta\theta_s$ is the temperature difference between the surface and the residual layer, which can be expressed in terms of the F_H and the scale height as shown at the right hand side. Furthermore, the scale height is given by

$$H_e = a V_{RL}^{3/4} \sqrt{t}, \quad (2)$$

where V_{RL} the residual layer wind speed, t the time since the day-night transition, and a = 0.15 m$^{1/4}$ s$^{1/4}$ is a numerical constant.

[10] It is important to note that in the simple first-order analysis by PM05 (with the main focus on the response of θ to a change in F_H), F_H is prescribed independently from the wind speed and the θ profile. PM05 required F_H/H_e to be the total flux divergence over the SBL depth in order to focus on the relation of the temperature trends as a function of wind speed. This total flux divergence would include both the turbulent and radiative flux. However, in reality from both ABL theory and observations, F_H as well as the radiative flux divergence depends interactively on both the wind speed and the stratification [e.g., *Derbyshire*, 1999].

[11] To illustrate the observed dependence F_H on wind speed, Figure 1 shows the observed nighttime F_H versus the 10 m wind speed from the CASES-99 experimental campaign over a prairie grassland [*Poulos et al.*, 2002; *Hartogensis and de Bruin*, 2005]. It is immediately clear that F_H is a function of wind speed. The CASES-99 observational setting is quite smooth (roughness length ~0.03 m). A site with a larger roughness would likely have fluxes to the left of the CASES-99 but still a function of wind speed.

[12] Figure 1 also indicates that two regimes are found, one where the magnitude of F_H increases with wind speed, and one where it decreases with wind speed. Thus, while the PM05 study may have instructive uses, the case discussed by PM05 (their Table 1) with the same prescribed F_H of −50 W m^{-2} for wind speeds of 1 m s^{-1} and 10 m s^{-1} cannot be realized in nature. It might be representative of a single wind speed over a rough surface. In fairness, the PM05 study was a sensitivity study in which they examined the response of the profile to a constant heat input for a range of wind speeds.

[13] The profiles in equation (1) were in part based on observations and they provide a first-order characterization of a nighttime θ profile. However, they do not explicitly account for the internal ABL dynamics, for feedbacks with

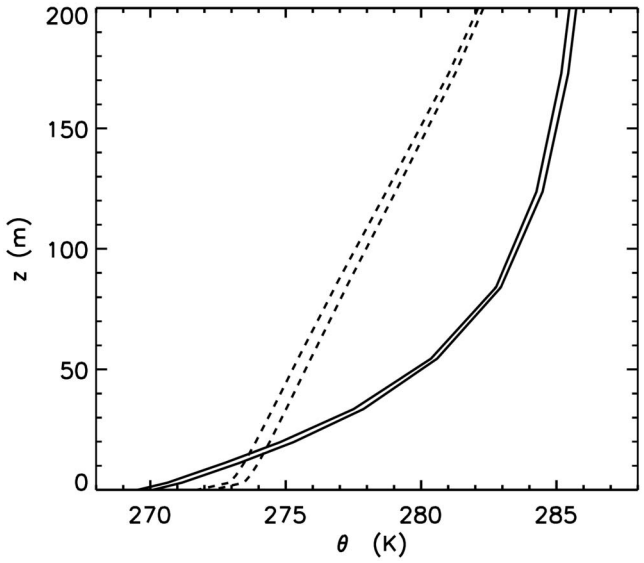

Figure 2. Potential temperature profiles after 18 simulation hours (0800 LST) for $\mathbf{V_g}$ = 2 m s^{-1} (solid lines) and $\mathbf{V_g}$ = 9 m s^{-1} (dashed lines) for the reference run and for increased longwave forcing by 40% CO_2 increase.

the land surface, and for radiation divergence. All of these processes can change the shape and behavior of the SBL, especially for calm conditions [*Steeneveld et al.*, 2006] (hereinafter referred to as S06).

3. Model and Experimental Setup

[14] To further study the vertical structure of the temperature increase during clear nights, we use a high-resolution atmospheric column model which accounts for turbulent mixing, longwave flux divergence and a full coupling with the land surface.

3.1. Model Description

[15] To calculate the temperature increase for enhanced radiative forcing, we utilize the single column model by *Duynkerke* [1991] (hereinafter referred to as D91). This model has been validated by S06 for a series of contrasting nights (both calm and windy) for the CASES-99 experiment, and against Cabauw tower observations in D91. The turbulent transport is estimated by a local diffusion approach, which has been proven a suitable method in the SBL [*Nieuwstadt*, 1984]. The eddy diffusivity K_x is given by first-order closure

$$K_x = \frac{l^2}{\phi_m \phi_x} \left| \frac{\partial \vec{V}}{\partial z} \right|, \tag{3}$$

with $l = k\,z$ as a first approximation and $x = m$, h, and q for momentum, heat, and humidity, respectively, and k is the Von Kármán constant, taken 0.4. Furthermore we use

$$\phi_x\left(\frac{z}{L}\right) = \frac{kz}{X_*}\frac{\partial \overline{X}}{\partial z} = 1 + \beta_x \frac{z}{L}\left(1 + \frac{\beta_x}{\alpha_x}\frac{z}{L}\right)^{\alpha_x - 1}, \tag{4}$$

with $L = -\overline{\theta} u_{*L}^3/(kgF_H)$ the local Obukhov length, with u_{*L} the local friction velocity. The coefficients $\beta_m = \beta_h = 5$ and $\alpha_m = \alpha_h = 0.8$ were derived for CASES-99 in S06, although it is important to realize that the uncertainties for z/L and ϕ_m and ϕ_h are relatively large, especially for very stable conditions [e.g., *Grachev et al.*, 2007; *Park et al.*, 2009].

[16] The vegetation surface temperature (T_{veg}) is computed from the surface energy budget residue:

$$C_v \frac{\partial T_{veg}}{\partial t} = Q^* - G - H - L_v E \tag{5}$$

where Q^* is the net radiation; H and L_vE are the sensible and latent heat flux (in W m^{-2}), respectively; and C_v is the heat capacity of the vegetation per unit of area. Finally G is the soil heat flux, which is calculated as $G = \Lambda\,(T_{veg} - T_{s,0})$, with $T_{s,0}$ the soil temperature of the topsoil and Λ the land surface coupling coefficient.

[17] Heat transport by longwave radiation is calculated by a broadband gray body emissivity scheme that accounts for the absorbing properties of water vapor, liquid water and CO_2 [*Garratt and Brost*, 1981]. In the soil (75 cm vertical increments at high vertical resolution) the model solves the diffusion equation. The required numerical values for the soil thermal diffusivity $\kappa = 0.155 \times 10^{-6}$ m^2 s^{-1}, land surface coupling coefficient Λ = 5.0 W m^{-2} K^{-1}, and C_v = 2000 J m^{-2} K were taken from observations from CASES-99 and Cabauw (S06). For more detailed description of the model, we refer to D91 and S06. We utilize 100 logarithmically distributed model layers in a vertical domain of 10 km and a time step of 60 s.

[18] The essential difference between the column model used in this study and the PM05 model (section 2) is that PM05 prescribe F_H while the column model interactively calculates the value of F_H based on the atmospheric temperature profile. Following equation (5), a change in T_{veg} will alter F_H, and this will consequently alter T_{veg}, and hence F_H again. Also, a change of T_{veg} will alter the soil heat flux G which will modify T_{veg} via equation (5) as well.

3.2. Experimental Setup

[19] In our model study we use information of the clear night of 23–24 October 1999 during the CASES-99 campaign. For this night we run the model and analyze the structure of the near surface temperature increase as function of geostrophic wind $\mathbf{V_g}$. The initial profile was inspired from the radiosonde of 23 October, 1900 UTC, with an approximately constant θ = 284 K from the surface to z = 800 m, and an inversion aloft. Specific humidity was taken constant (1.0 g kg^{-1}) in the whole model domain for the default experiment. The initial wind speed was constant with height and equal to the $\mathbf{V_g}$, but matching a logarithmic profile close to the surface.

[20] All model runs are first performed for a uniform tropospheric CO_2 concentration of 330 ppm and then repeated for increased values for the tropospheric CO_2 concentration of 40%. This modification results in a net change in downward longwave flux of ~4.8 W m^{-2}. Current calculations have been repeated using an increased specific humidity in the ABL rather than a CO_2 increase. These experiments provide a similar structure of vertical distribution of temperature increase as will be presented below for CO_2 increase. Water vapor increases have also been found to alter the long-term trends of surface temperatures, and

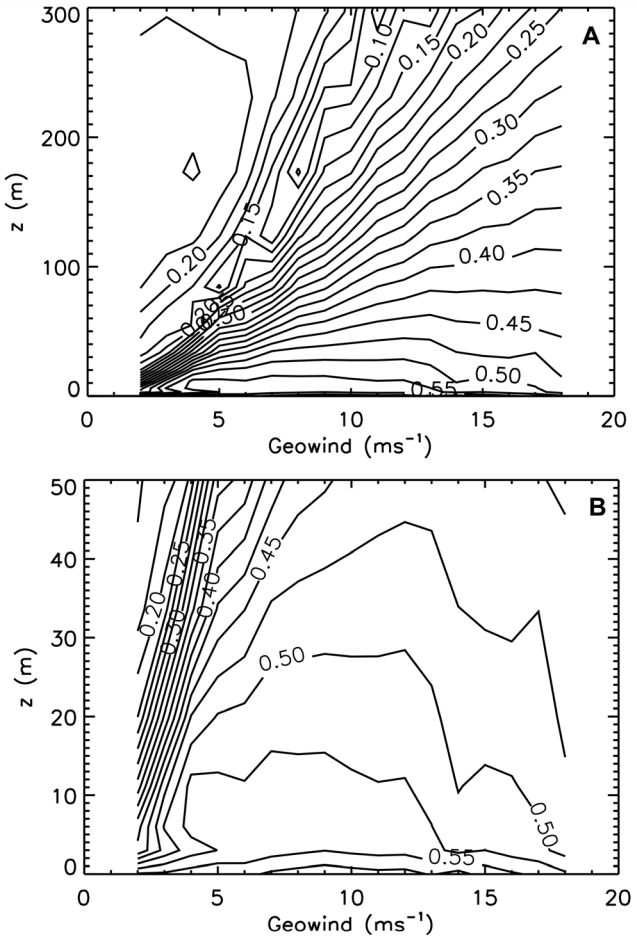

Figure 3. Modeled vertical distribution of potential temperature increase due to 40% CO_2 concentration increase (from 330 to 460 ppm). The plot shows 0600 LST (after 16 h of model simulation), with land surface coupling coefficient = 5.0 W m^{-2} K^{-1}, for (a) 0–300 m and (b) 0–50 m.

appears to be the major cause of surface warming during winter, particularly at higher elevations [*Rangwala et al.*, 2009].

4. Results and Discussion

[21] Figure 2 shows the model results for potential temperature profile of θ at the end of the night for two values of geostrophic wind $\mathbf{V_g}$ (namely, 2 and 9 m s^{-1}) and for the two values of CO_2 concentrations (namely, 330 and 460 ppm). For the calm nights ($\mathbf{V_g}$ = 2 m s^{-1}), we note the typical strong negative curvature over the whole ABL depth which is also consistent with equation (1). For the windy nights, the profile is only negatively curved close to the surface and positively curved aloft [see also *Estournel and Guedalia*, 1985; *Edwards et al.*, 2006]. The shape of the profile in each wind class is similar for all increased CO_2 concentrations. Furthermore, we see that the θ increase for enhanced CO_2 concentrations decreases with height (in particular for the low winds).

[22] Figure 3 shows the modeled θ increase resulting from a 40% CO_2 concentration increase for the (z, $\mathbf{V_g}$) space. The results are based on calculations for the end of the night (0600 LST, after 16 simulation hours) as a function of $\mathbf{V_g}$ ($2 < \mathbf{V_g} < 18$ m s^{-1}) and as a function of height (until 300 m in Figure 3a and until 50 m in Figure 3b). It is clearly seen that the near surface temperature increase is not strongly dependent on geostrophic wind speed in the range $5 < \mathbf{V_g} < 15$ m s^{-1} which is confirmed in Figure 4 which shows the 2 m temperature increase as function of $\mathbf{V_g}$ and 10 m wind speed V_{10}. For $2 < V_{10} < 4$ m s^{-1} the 2 m temperature increase is rather constant at approximately 0.58 K.

[23] Several aspects of the SBL physics can explain the model behavior in Figures 3 and 4. However, it is important to report first that the model was able to approximately reproduce the behavior for F_H versus U_{10} as observed in Figure 1 (not shown). The first aspect of SBL physics to be considered is the SBL height over which the additional heating is distributed. Higher geostrophic wind speeds result in deeper boundary layers and as such we could expect a smaller 2 m temperature increase for larger $\mathbf{V_g}$. However, a smaller temperature increase for larger $\mathbf{V_g}$ is only seen for

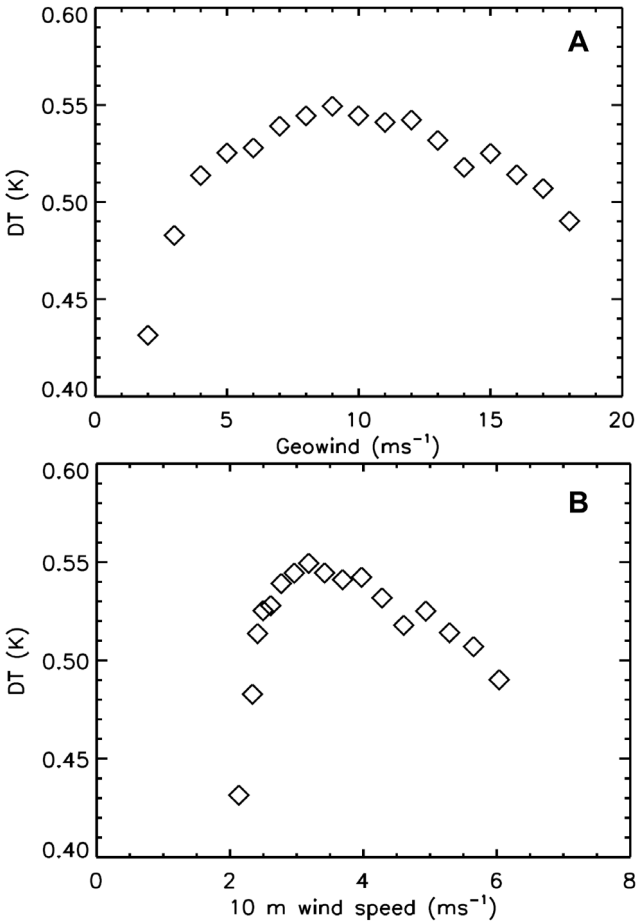

Figure 4. Modeled 2 m potential temperature increase due to 40% CO_2 concentration increase (from 330 to 460 ppm) as function of (a) geostrophic wind speed and (b) 10 m wind speed. The plot shows the results for 0600 LST (after 16 h of model simulation), with land surface coupling coefficient = 5.0 W m^{-2} K^{-1}.

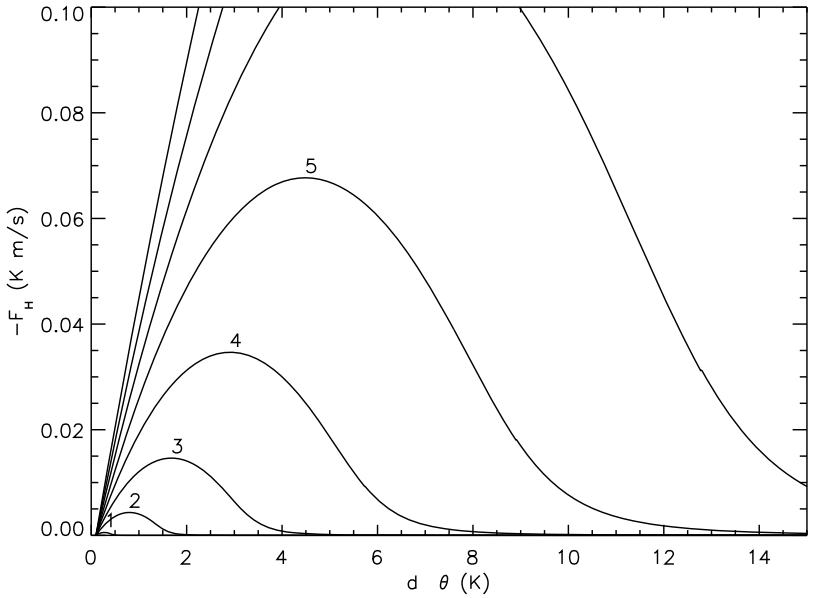

Figure 5. Surface sensible heat fluxes F_H as function of temperature difference between the vegetation surface and the 2 m level (dθ) for different values (printed at the top of the curves) of the 10 m wind speed (in m s^{-1}), based on the flux profile relationships given by *Duynkerke* [1991] and adopted from *Holtslag et al.* [2007].

$\mathbf{V_g}$ > 15 m s^{-1}, and hence the impact of the boundary layer depth is apparently only dominant in this region.

[24] For $\mathbf{V_g}$ < 5 m s^{-1}, the near surface wind speed is small, which means that the turbulence intensity and hence F_H is small as well. Hence, increased longwave downwelling radiation will increase the surface vegetation temperature, but this can hardly be compensated by the sensible heat flux due to the weak turbulence intensity. Consequently, for these low wind speeds the increase of T_{veg} reduces the soil heat flux, and the increased heat input propagates to the soil rather than to the atmosphere. Therefore, the increase of 2 m temperature decreases for low wind speeds.

[25] To explain the model behavior in the intermediate regime, Figure 5 shows F_H as function of the temperature difference between the vegetation surface and the 2 m level, for different values of the 10 m wind speed, using the flux profile relationships in D91 [after *Holtslag et al.*, 2007]. For a constant wind speed, the two regimes that were mentioned earlier are evident. For the weakly stable boundary layer (left of the maximum magnitude of F_H) the magnitude of F_H increases with increasing stratification, while in the strongly stable boundary layer the magnitude of F_H decreases with stratification.

[26] For the very stable regime where turbulence is still active, the increased radiative forcing will weaken the near surface stratification, which will subsequently increase the magnitude of F_H, and via equation (5) also T_{veg}. As such this magnifies the effect of enhanced CO_2. This also explains the steep gradient of temperature increase at $\mathbf{V_g}$ = 4 m s^{-1} in Figure 3b.

[27] Also in the weakly stable regime (left of peak in Figure 5), the increased downward radiation will decrease the near surface stratification, but in this regime the magnitude of F_H is reduced and thus the warming is inhibited by sufficient turbulence to remove the added heat from the surface. In addition, the compensation is stronger for higher wind speeds, since the isolines in Figure 5 steepen further to the left. As a whole, this means that compensating mechanisms keep the temperature increase at screen level relatively constant!

[28] The finding that the near surface temperature increase is approximately constant for 5 < $\mathbf{V_g}$ < 15 m s^{-1}, corresponds to the findings by *Parker* [2004] although one should keep in mind that the latter study also covered differences between temperature rise in rural and urban areas. It also appears that destabilization of the SBL by the added heat can lead to a deeper turbulent boundary layer [*Walters et al.* 2007]. This in turn entrains warmer air to the surface. Thus, there is additional heating at the surface due to a redistribution of heat. This is further examined by R. T. McNider et al. (Sensitivity of the nocturnal boundary layer to changes in radiative forcing, submitted to *Journal of the Atmospheric Sciences*, 2010).

[29] Note that in our model calculations the difference in 2 m temperature increase is only 0.12 K if we vary the $\mathbf{V_g}$ between 2 and 10 m s^{-1}. PM05 find a much larger difference of 1.3 K difference with their approach, mostly because they ignore the land surface-vegetation-atmosphere feedback. This is despite the fact that changes in incoming energy are greater than the 1 W m^{-2} change included by PM05. In an additional experiment with the present model, utilizing Λ = 0 (and as such decoupling from the surface), we found a temperature rise of 0.8 K over a broad range of $\mathbf{V_g}$, which is much closer to the 1.3 K in PM05 (not shown). The remaining difference is highly likely due to differences the formulations of the two models.

[30] We would like to stress that the current quantitative findings are not representative for the global scale, because the temperature increase for the global scale is found by

integrating the model on a global scale for a long time, allowing for feedbacks with clouds, the land surface vegetation, and other aspects. We also would like to remark that *Parker* [2004] based his classification on near surface wind speed. The near surface wind speed, in principle, depends on the SBL stability itself, and is calculated in the model. So, it could be that if the SBL stability changes due to different longwave forcing, the wind speed is also altered. Increased forcing might result in reduced stability and increased near surface wind speed, so that some nights may jump from the calm night class to the windy night class [*Walters et al.*, 2007].

[31] Our more complete model does support the PM05 result that the response to a change in surface forcing is a strong function of height. Thus, PM05 made a good point when they raise the question whether screen level observations are a good measure for assessing long-term temperature increase. Perhaps an integral measure over the SBL (as in S06) might be more suitable. Note that radiosondes often lack the vertical resolution close to the surface to resolve the structure in the SBL as sketched above.

5. Conclusion

[32] In this paper we revisit the issue of land surface temperature trends and their dependence on wind speeds. In an earlier study, *Pielke and Matsui* [2005] concluded that the nighttime 2 m temperature increase due to changes in longwave flux divergence should strongly depend on wind speed. Here we conclude that the model used in that study is not sufficient for such an analysis because of the limited processes represented as well as not considering the land surface-vegetation-atmosphere feedback

[33] Different than *Pielke and Matsui* [2005], the current study uses a high-resolution column model that covers more of the relevant physics, i.e., turbulent mixing, radiative heat transport and heat flux from the soil, to assess the question whether long-term near surface temperature increases should differ between calm and windy nights. Hence, this study accounts for feedbacks between the surface vegetation temperature and the soil on one hand, and for internal feedbacks between near surface stratification and the sensible heat flux on the other hand, while both were missing in the study by *Pielke and Matsui* [2005]. We find that the temperature increase close to the surface is much less sensitive to wind speed than suggested by PM05 when the longwave radiative forcing change is from increases in the atmospheric concentration of CO_2. However, the temperature changes do depend on height as also suggested by PM05.

[34] Thus our findings appear to support the earlier findings by *Parker* [2004] who found that the temperature increase from observations (ascribed to greenhouse gases) is rather independent from wind speed. However, we note that in the SBL surface wind speed and stability are interrelated. Using actual wind speeds as did *Parker* [2004], is not the same as the geostrophic winds used here and implicitly in PM05. In addition, the forecasted temperature increase does depend on the degree of atmosphere land coupling. This illustrates that climate models should properly account for this interaction to provide reliable results.

[35] Finally, we note that the *Parker* [2004] conclusion that urban and land use effects were not seen in the observed trends when grouped by wind speed, explicitly rely on past studies [*Johnson et al.*, 1991] that indicated that urban heat island effects were larger at low wind speeds. Our model results indicate that factors such as radiative forcing or land use change, which might change surface energy balances, still rely on wind speed and land surface interaction to transfer heat from the surface to shelter level.

[36] Our study shows that the competing effects of boundary layer height and wind speed–dependent fluxes yield changes in shelter temperature that are largely independent of wind speed. PM05 only considered the role of wind speed and boundary layer height. It is likely that urban heat island effects as observed, are due to the resident time of a parcel of air over a city and not due to the flux changes considered here or in PM05. Furthermore, the parameter spaces investigated in this paper are limited. For example, the CASES-99 observational site simulated here is quite smooth (the roughness length used in the simulations was 0.03 m). It is possible that larger roughnesses might provide more sensitivity to wind speed. This will be further explored by McNider et al. (submitted manuscript, 2010).

[37] Finally, we agree with PM05 that additional work is needed to understand SBL responses to both land use change and radiative forcing. *Klotzbach et al.* [2009], for example, who show a statistically significant divergence between the long-term trends of the surface air and lower tropospheric temperatures at higher latitudes in the winter, indicate that the changes in the SBL over time remains an important climate change issue that has been not yet completely examined and understood.

[38] **Acknowledgments.** We thank O. K. Hartogensis for gathering CASES-99 observations (as shown in Figure 1) and A. Overeem and B. J. H. van de Wiel for valuable comments on earlier versions of the manuscript. Partial support from R. Pielke Sr. was provided by the University of Colorado at Boulder Vice Chancellor for Research. We also acknowledge three anonymous reviewers for their very useful comments and suggestions.

References

Chimonas, G., and C. J. Nappo (1989), Wave drag in the planetary boundary layer over complex terrain, *Boundary Layer Meteorol.*, *47*, 217–232, doi:10.1007/BF00122330.

Delage, Y., P. A. Barlett, and J. H. McCauchy (2002), Study of 'soft' night time surface layer decoupling over forest canopies in a land-surface model, *Boundary Layer Meteorol.*, *103*, 253–276, doi:10.1023/A:1017443021557.

Derbyshire, S. H. (1999), Boundary layer decoupling over cold surfaces as a physical boundary instability, *Boundary Layer Meteorol.*, *90*, 297–325, doi:10.1023/A:1001710014316.

Duynkerke, P. G. (1991), Radiation fog: A comparison of model simulation with detailed observations, *Mon. Weather Rev.*, *119*, 324–341, doi:10.1175/1520-0493(1991)119<0324:RFACOM>2.0.CO;2.

Edwards, J. M., R. J. Beare, and A. J. Lapworth (2006), Simulation of the observed evening transition and nocturnal boundary layers: Single column modelling, *Q. J. R. Meteorol. Soc.*, *132*, 61–80, doi:10.1256/qj.05.63.

Estournel, C., and D. Guedalia (1985), Influence of geostrophic wind on atmospheric nocturnal cooling, *J. Atmos. Sci.*, *42*, 2695–2698, doi:10.1175/1520-0469(1985)042<2695:IOGWOA>2.0.CO;2.

Folland, C. K., et al. (2001), Observed climate variability and change, in *Climate Change 2001: The Scientific Basis. Contribution of Working Group I to the Third Assessment Report of the Intergovernmental Panel on Climate Change*, edited by J. T. Houghton et al., pp. 99–181, Cambridge Univ. Press, Cambridge, U. K.

Garratt, J. R., and R. A. Brost (1981), Radiative cooling effects within and above the nocturnal boundary layer, *J. Atmos. Sci.*, *38*, 2730–2746, doi:10.1175/1520-0469(1981)038<2730:RCEWAA>2.0.CO;2.

Grachev, A. A., E. L. Andreas, C. W. Fairall, P. S. Guest, and P. O. G. Persson (2007), SHEBA flux-profile relationships in the stable atmospheric boundary layer, *Boundary Layer Meteorol.*, *124*, 315–333, doi:10.1007/s10546-007-9177-6.

Ha, K. J., and L. Mahrt (2003), Radiative and turbulent fluxes in the nocturnal boundary layer, *Tellus, Ser. A*, *55*, 317–327, doi:10.1034/j.1600-0870.2003.00031.x.

Hartogensis, O. K., and H. A. R. de Bruin (2005), Monin-Obukhov similarity functions of the structure parameter of temperature and turbulent kinetic energy dissipation rate in the stable boundary layer, *Boundary Layer Meteorol.*, *116*, 253–276, doi:10.1007/s10546-004-2817-1.

Holtslag, A. A. M., G. J. Steeneveld, and B. J. H. van de Wiel (2007), Role of land-surface feedback on model performance for the stable boundary layer, *Boundary Layer Meteorol.*, *125*, 361–376, doi:10.1007/s10546-007-9214-5.

Johnson, G. T., T. R. Oke, T. J. Lyons, D. G. Steyn, I. D. Watson, and J. A. Voogt (1991), Simulation of surface urban heat islands under "ideal" conditions at night. Part 1: Theory and tests against field data, *Boundary Layer Meteorol.*, *56*, 275–294, doi:10.1007/BF00120424.

Klotzbach, P. J., R. A. Pielke Sr., R. A. Pielke Jr., J. R. Christy, and R. T. McNider (2009), An alternative explanation for differential temperature trends at the surface and in the lower troposphere, *J. Geophys. Res.*, *114*, D21102, doi:10.1029/2009JD011841.

McNider, R. T., and R. A. Pielke (1981), Diurnal boundary layer development over sloping terrain, *J. Atmos. Sci.*, *38*, 2198–2212, doi:10.1175/1520-0469(1981)038<2198:DBLDOS>2.0.CO;2.

McNider, R. T., X. Shi, M. Friedman, and D. E. England (1995), On the predictability of the stable atmospheric boundary layer, *J. Atmos. Sci.*, *52*, 1602–1614, doi:10.1175/1520-0469(1995)052<1602:POTSAB>2.0.CO;2.

Nieuwstadt, F. T. M. (1984), The turbulent structure of the stable, nocturnal boundary layer, *J. Atmos. Sci.*, *41*, 2202–2216, doi:10.1175/1520-0469(1984)041<2202:TTSOTS>2.0.CO;2.

Park, S., S. Park, C. Ho, and L. Mahrt (2009), Flux-gradient relationship of water vapor in the surface layer obtained from CASES-99 experiment, *J. Geophys. Res.*, *114*, D08115, doi:10.1029/2008JD011157.

Parker, D. E. (2004), Large scale warming is not urban, *Nature*, *432*, 290, doi:10.1038/432290a.

Parker, D. E. (2006), A demonstration that large-scale warming is not urban, *J. Clim.*, *19*, 2882–2895, doi:10.1175/JCLI3730.1.

Pielke, R. A., Sr., and T. Matsui (2005), Should light wind and windy nights have the same temperature trends at individual levels even if the boundary layer averaged heat content change is the same?, *Geophys. Res. Lett.*, *32*, L21813, doi:10.1029/2005GL024407.

Poulos, G. S., et al. (2002), CASES-99: A comprehensive investigation of the stable nocturnal boundary layer, *Bull. Am. Meteorol. Soc.*, *83*, 555–581, doi:10.1175/1520-0477(2002)083<0555:CACIOT>2.3.CO;2.

Rangwala, I., J. Miller, G. L. Russell, and M. Xu (2008), Influence of increasing surface humidity on winter warming at high altitudes through the 21st century, *Eos Trans. AGU*, *89*(53), Fall Meet. Suppl., Abstract GC13B-03.

Steeneveld, G. J., B. J. H. van de Wiel, and A. A. M. Holtslag (2006), Modeling the evolution of the atmospheric boundary layer coupled to the land surface for three contrasting nights in CASES-99, *J. Atmos. Sci.*, *63*, 920–935, doi:10.1175/JAS3654.1.

Steeneveld, G. J., M. J. J. Wokke, C. D. Groot Zwaaftink, S. Pijlman, B. G. Heusinkveld, A. F. G. Jacobs, and A. A. M. Holtslag (2010), Observations of the radiation divergence in the surface layer and its implication for its parametrization in numerical weather prediction models, *J. Geophys. Res.*, *115*, D06107, doi:10.1029/2009JD013074.

Stull, R. B. (1983), A heat-flux history length scale for the nocturnal boundary layer, *Tellus, Ser. A*, *35*, 219–230, doi:10.1111/j.1600-0870.1983.tb00199.x.

Stull, R. B. (2000), *Meteorology for Scientists and Engineers*, 2nd ed., 502 pp., Brooks/Cole, Pacific Grove, Calif.

van de Wiel, B. J. H., A. F. Moene, R. J. Ronda, H. A. R. de Bruin, and A. A. M. Holtslag (2002), Intermittent turbulence and oscillations in the stable boundary layer over land. Part II: A system dynamics approach, *J. Atmos. Sci.*, *59*, 2567–2581, doi:10.1175/1520-0469(2002)059<2567:ITAOIT>2.0.CO;2.

Walters, J. T., R. T. McNider, X. Shi, W. B. Norris, and J. R. Christy (2007), Positive surface temperature feedback in the stable nocturnal boundary layer, *Geophys. Res. Lett.*, *34*, L12709, doi:10.1029/2007GL029505.

A. A. M. Holtslag and G. J. Steeneveld, Meteorology and Air Quality Section, Wageningen University, PO Box 47, NL-6700 AA Wageningen, Netherlands. (gert-jan.steeneveld@wur.nl)

R. T. McNider, Department of Atmospheric Science, University of Alabama in Huntsville, Huntsville, AL 35805, USA.

R. A. Pielke Sr., CIRES, University of Colorado at Boulder, Boulder, CO 80309, USA.